

*«From observation to discovery:
data analysis with a human brain»
IUSS seminar, Lecture 2*

Pavia, 2023 March 15

**The variable background
of XMM-Newton**

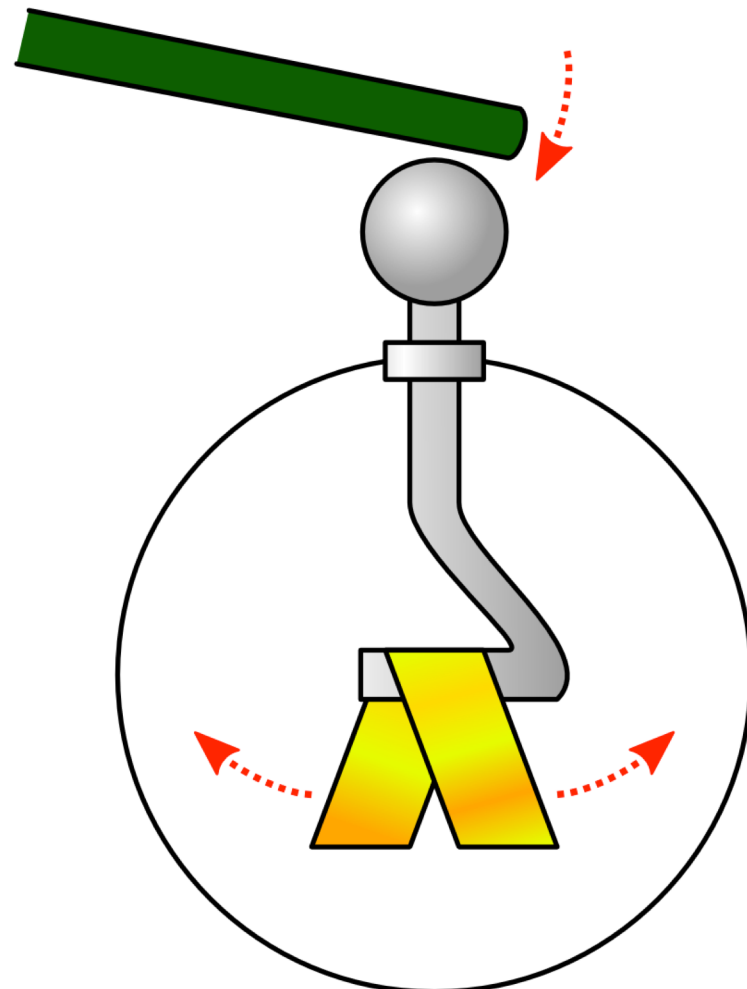
Andrea Tiengo

The discovery of Cosmic Rays

At the beginning of the 20th century, the **discharge rate** of an electroscope was used as a measure of the level of **radioactivity**

Electroscopes discharge slowly even in the absence of a radioactive source ⇒ **background radiation**

Radiation from radioactive materials in the Earth?



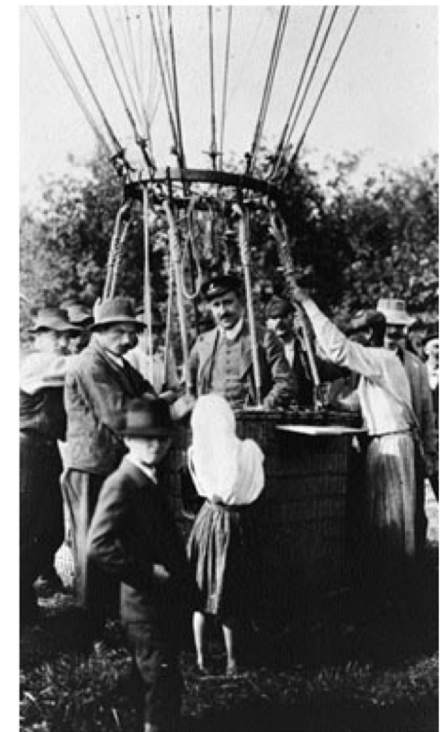
ELECTROSCOPE

The discovery of Cosmic Rays

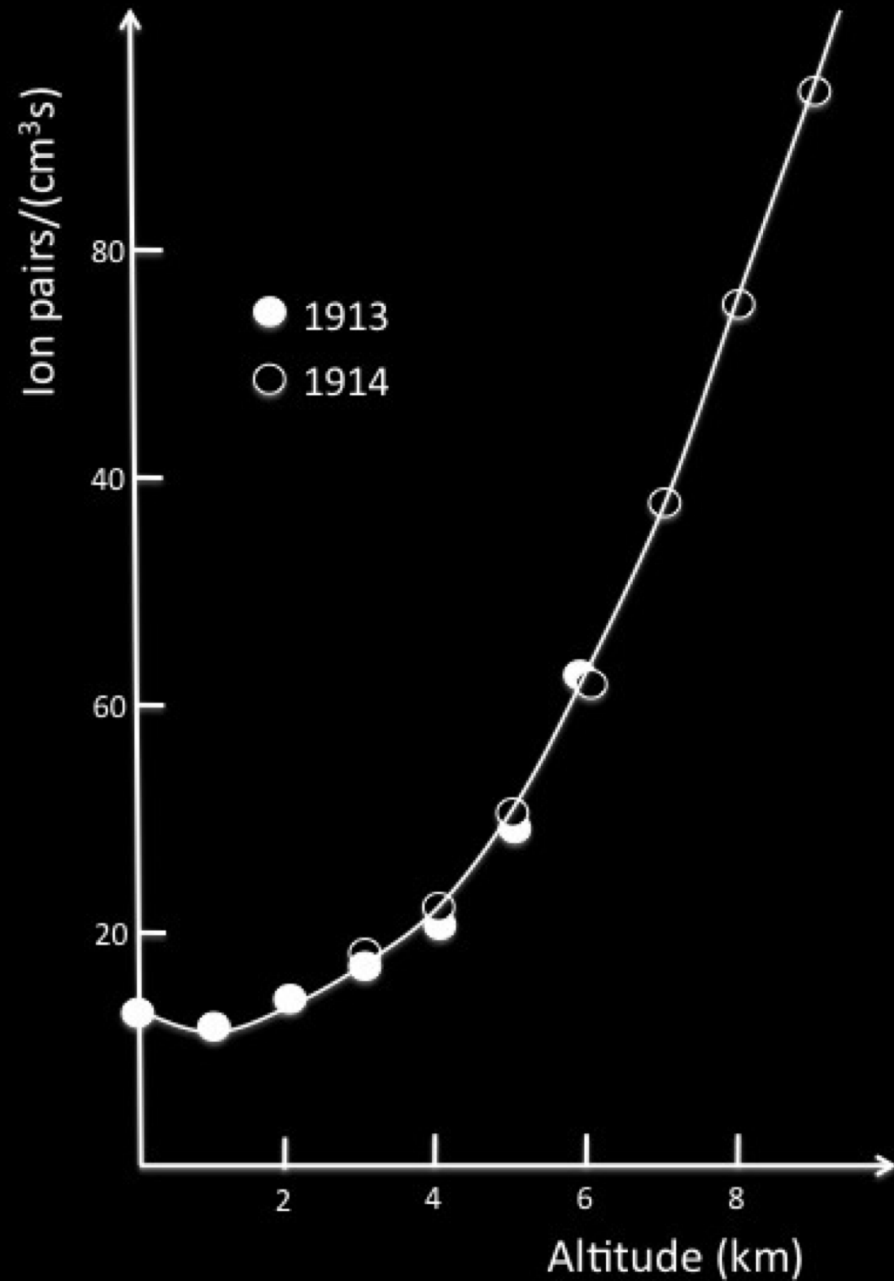
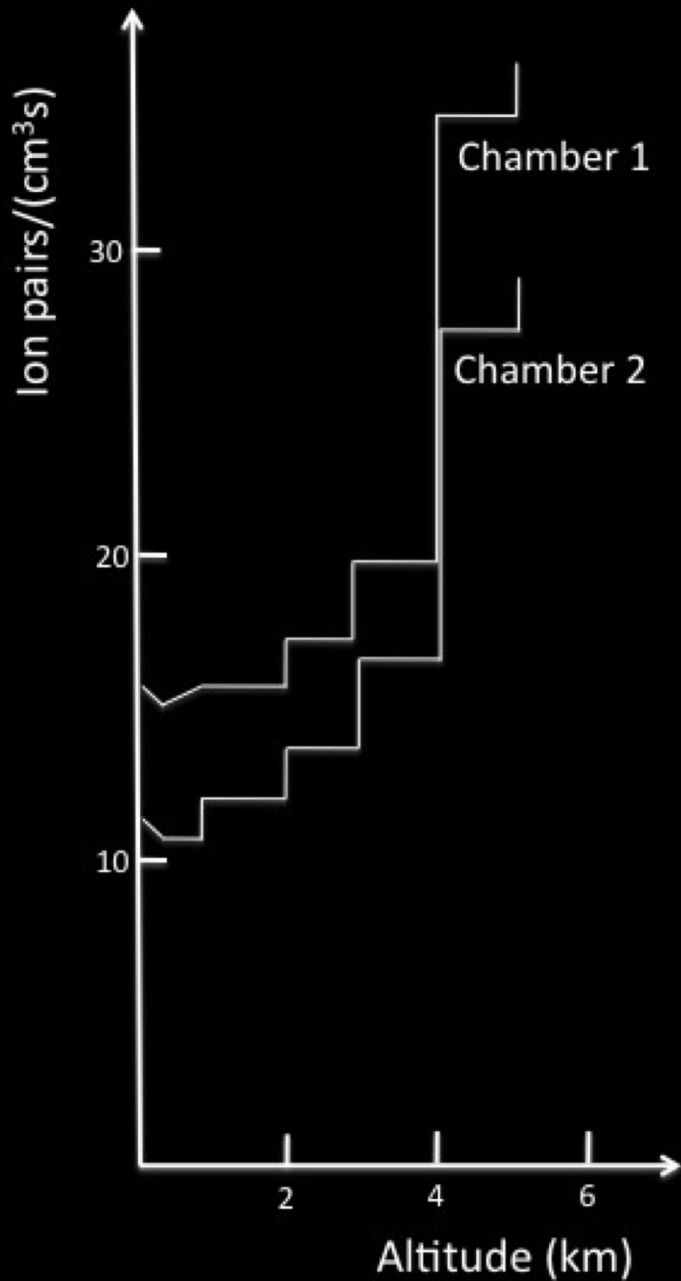
If due to radioactive materials in the Earth, the effect should diminish with height

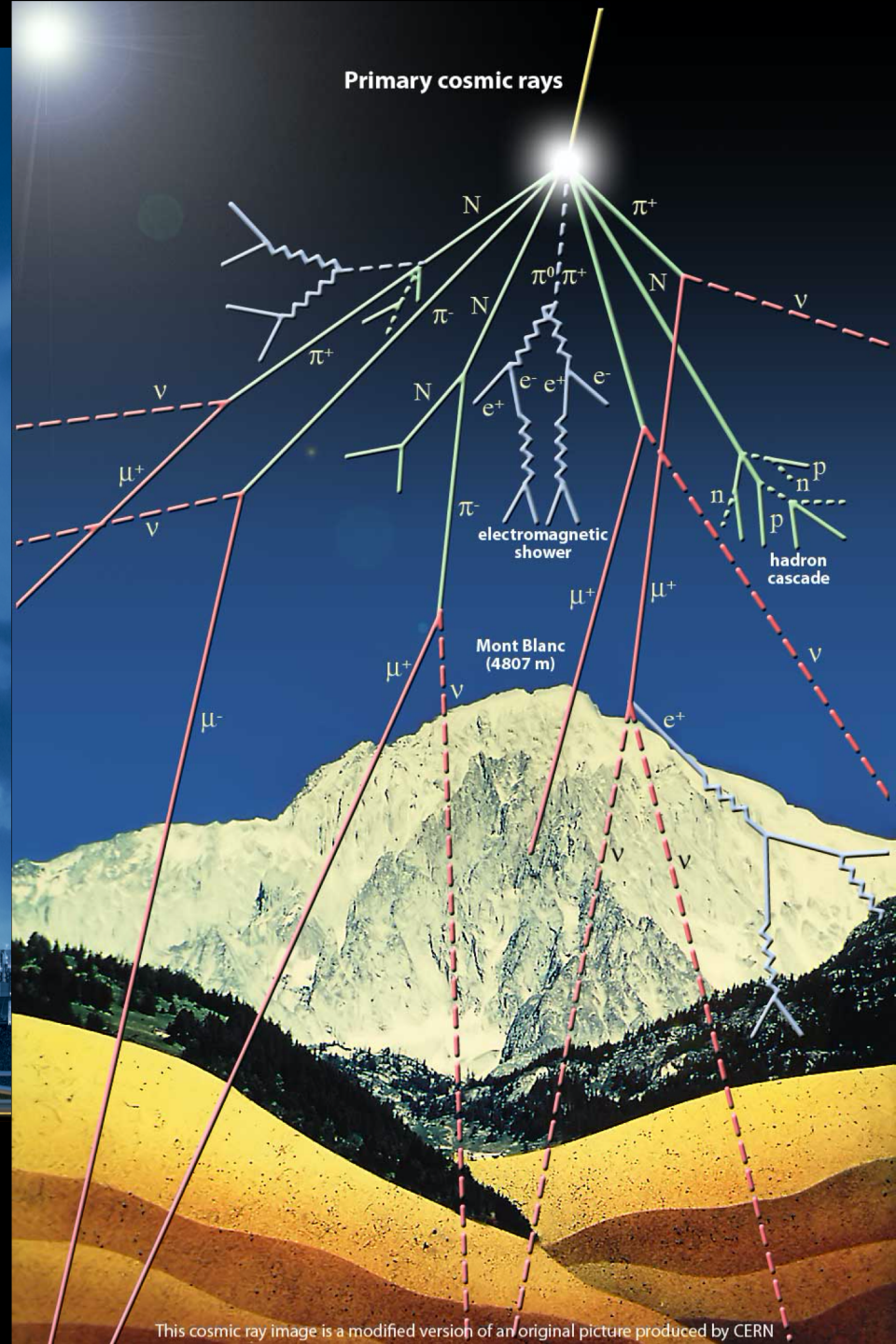
In 1912, during a balloon flight Victor Hess discovered that the effect was indeed **increasing with height**, and concluded that:

“a radiation of very high penetrating power enters our atmosphere from above”



V. Hess in 1912





What are Cosmic Rays?

- Cosmic rays particles hit the Earth's atmosphere at the rate of about **1000 per square meter per second**.
- They are ionized nuclei: about **90% protons**, 9% alpha particles and the rest heavy nuclei
- Most cosmic rays are **relativistic**, having energies comparable or somewhat greater than their masses.
- A very few of them have ultrarelativistic energies extending up to 10^{20} eV, 11 orders of magnitude greater than the equivalent rest mass energy of a proton.

The fundamental question of cosmic ray physics is:

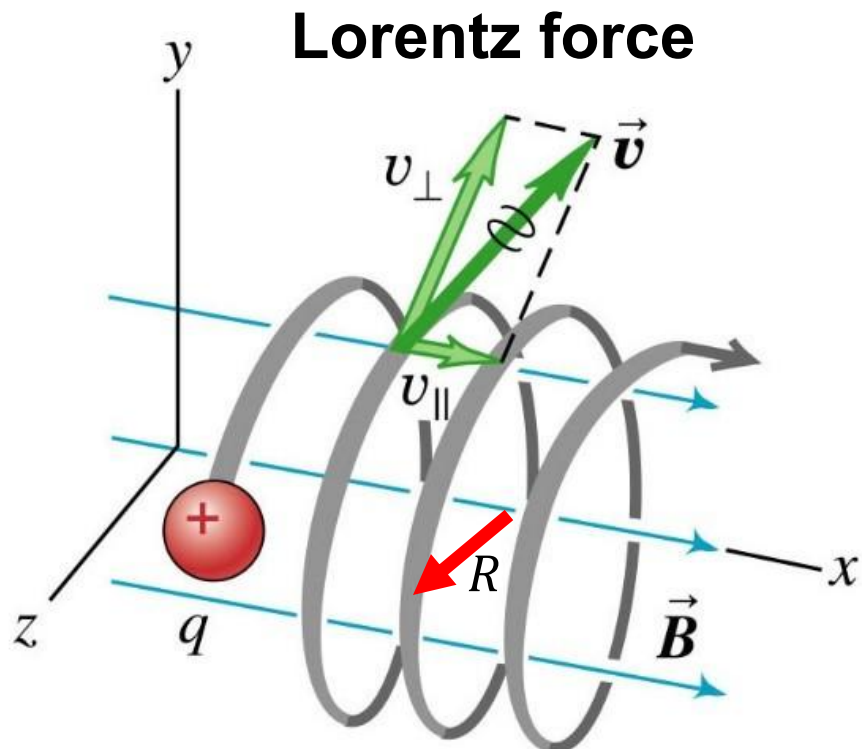
“Where do they come from?”

and in particular:

“How are they accelerated to such high energies?”

The origin of cosmic rays

The trajectory of **charged particles** is deflected by the (terrestrial, Galactic, intergalactic...) **magnetic field**



$$\vec{F} = q\vec{v} \times \vec{B}$$

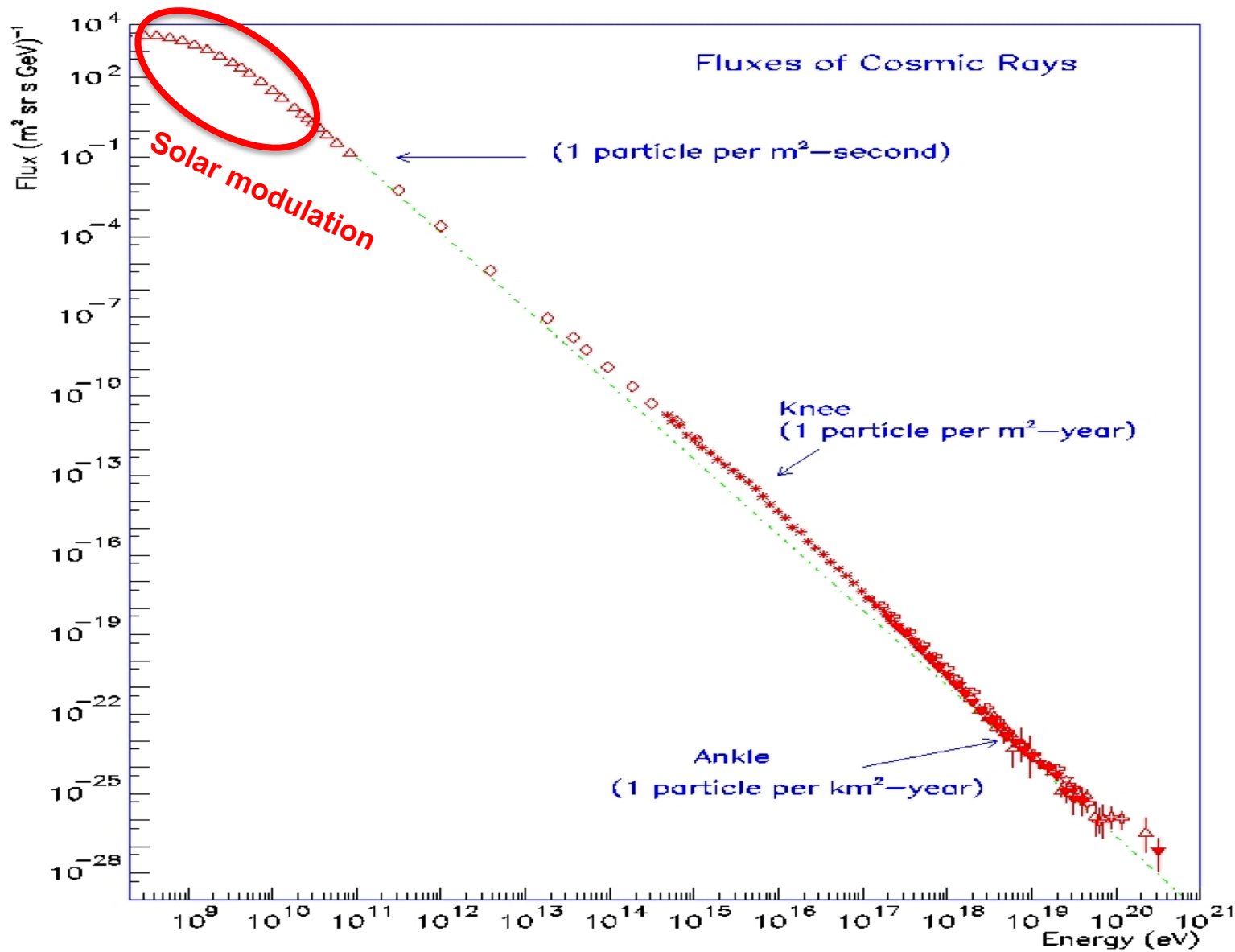
$$m \frac{v_{\perp}^2}{R} = qv_{\perp}B \Rightarrow R = \frac{mv_{\perp}}{qB}$$

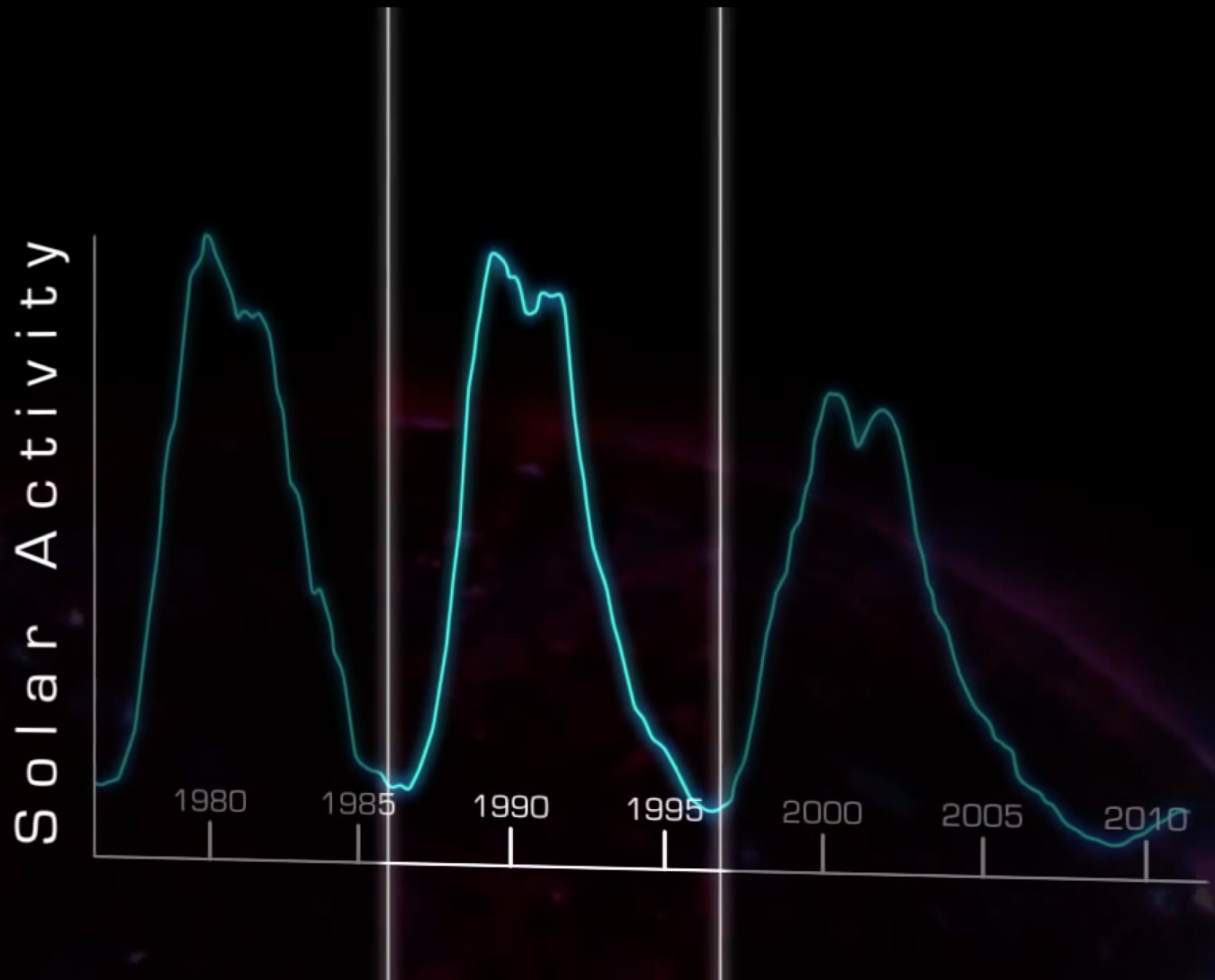
Curvature radius (R) is large
(\Rightarrow little deviation) only for
energetic particles (large v) and
weak magnetic fields (small B)

Copyright © 2004 Pearson Education, Inc., publishing as Addison Wesley.

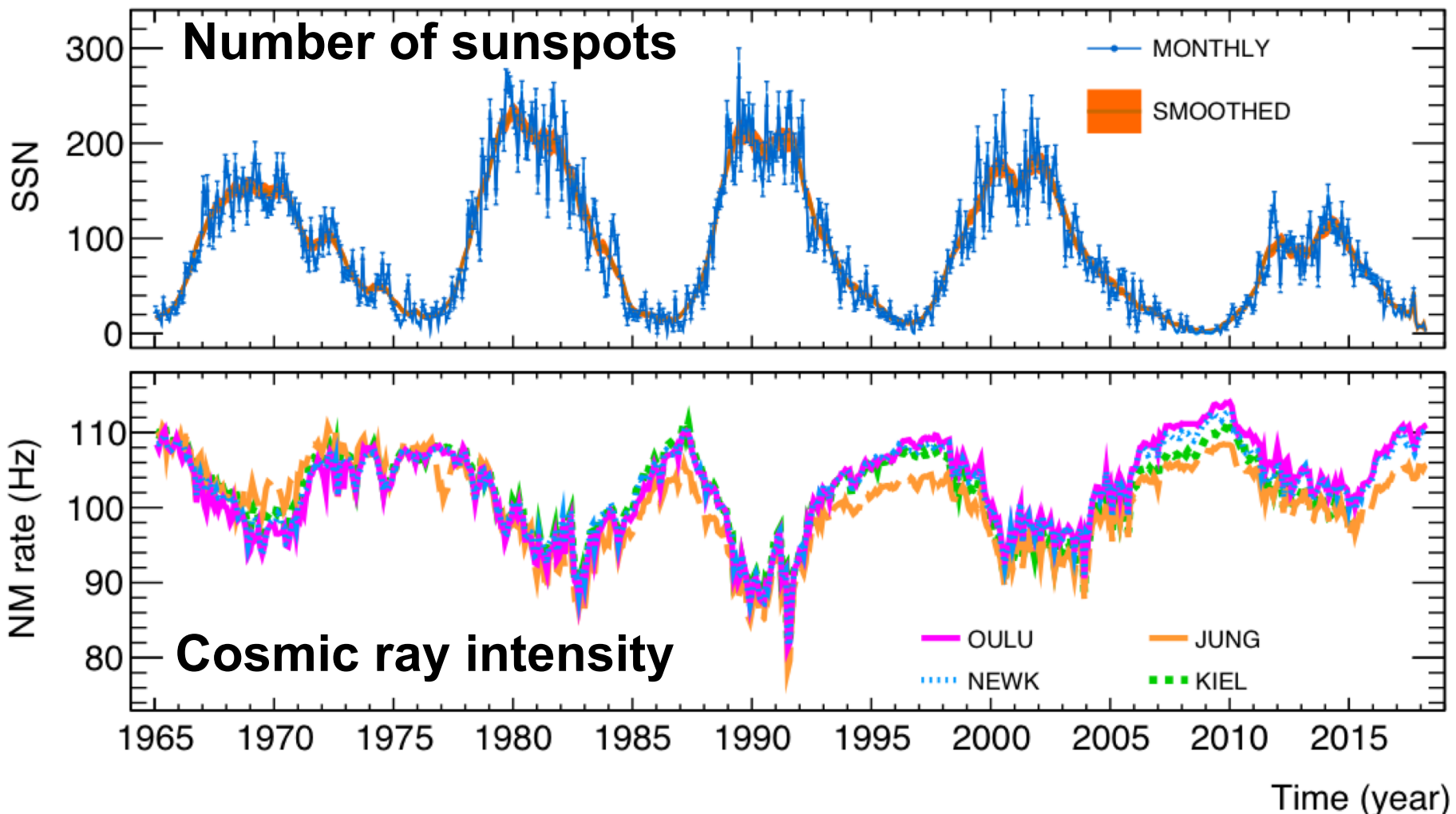
We can (roughly) identify only the source of charged particles with **ultrarelativistic energies** (Pierre Auger Observatory)

The (local) Cosmic Ray spectrum



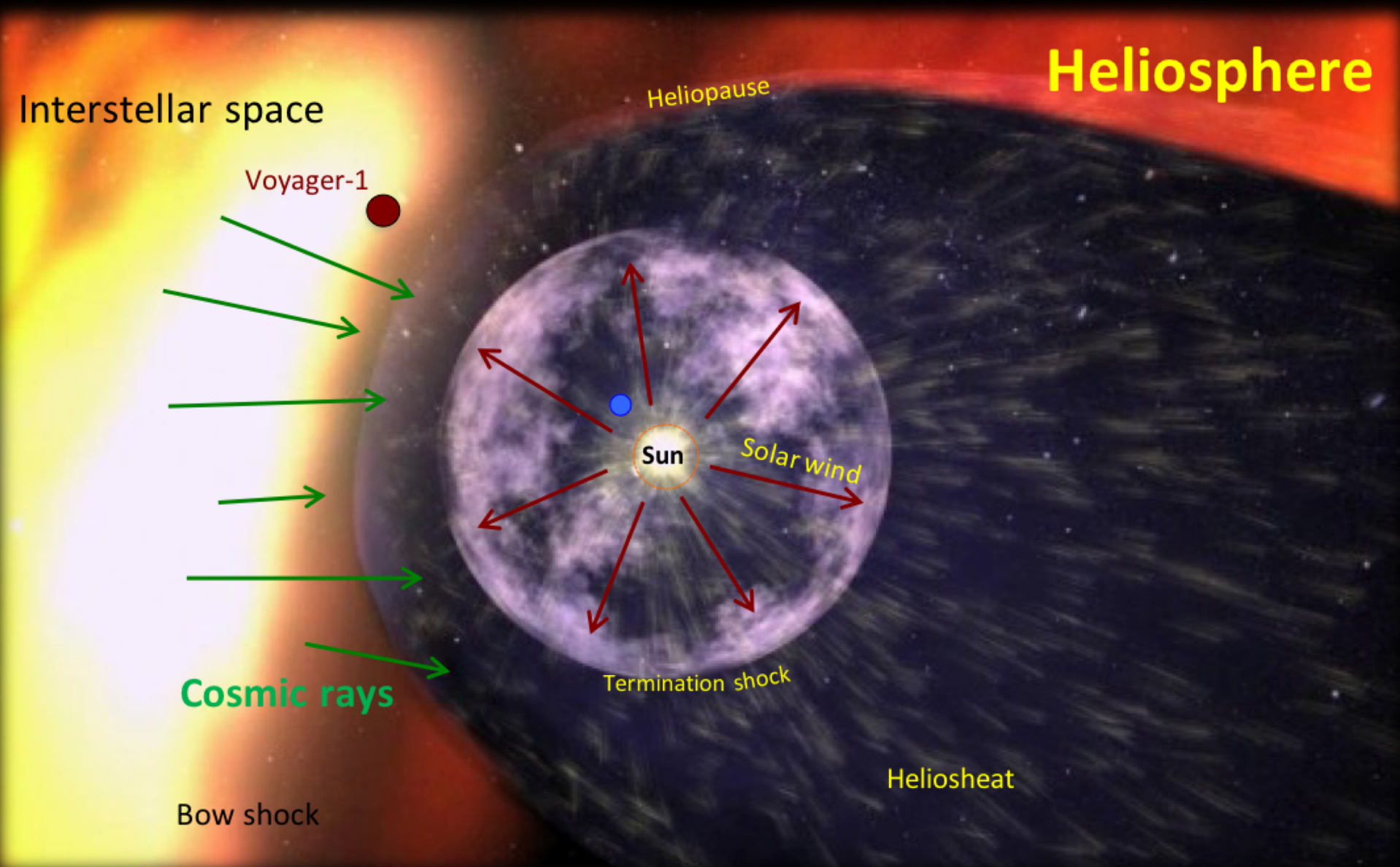


Solar modulation

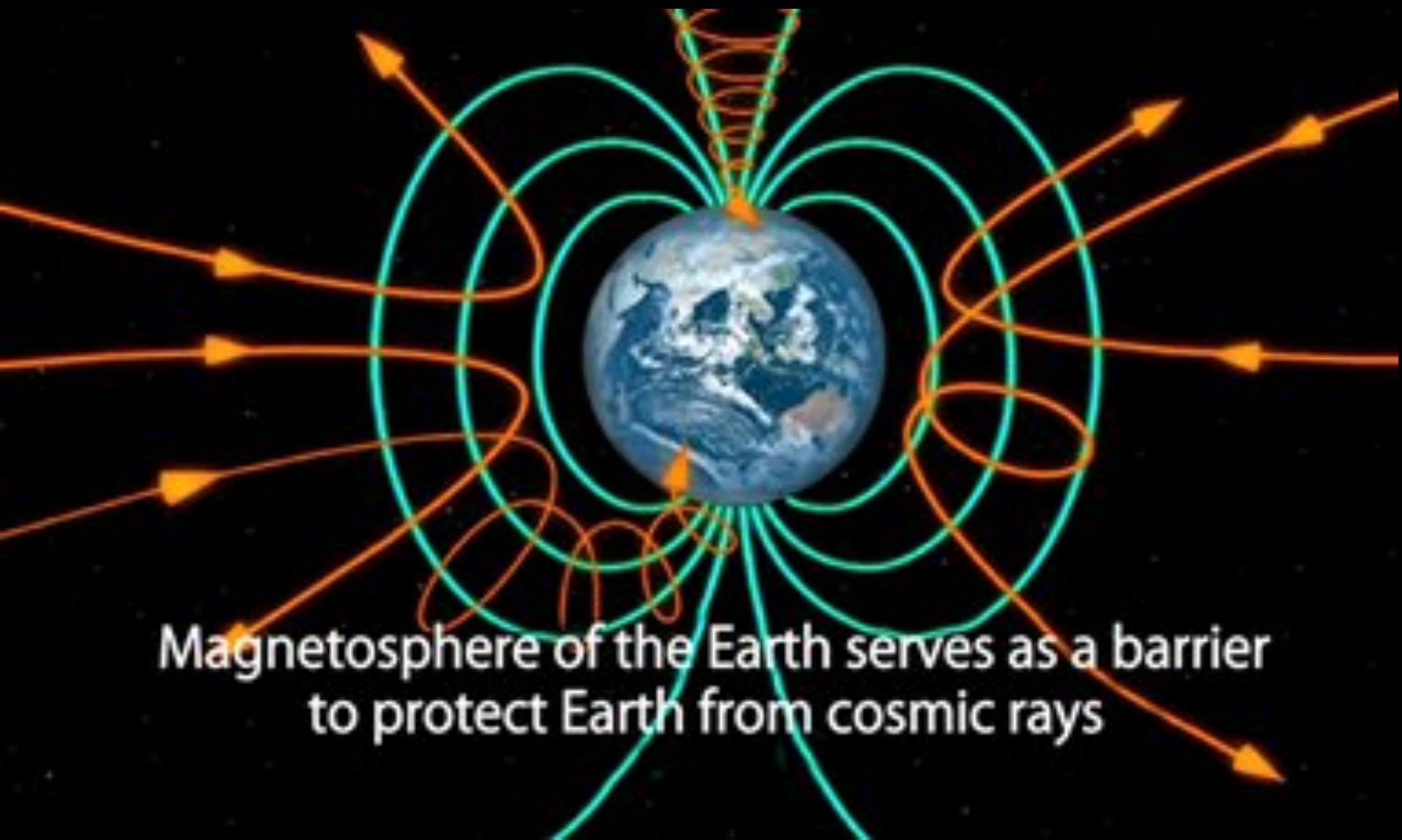


The intensity of low energy **cosmic rays** in the Solar System is **anti-correlated** to Sun activity (**11-years cycle**)

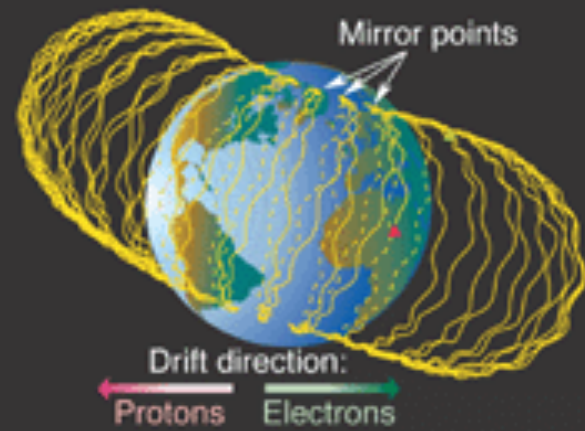
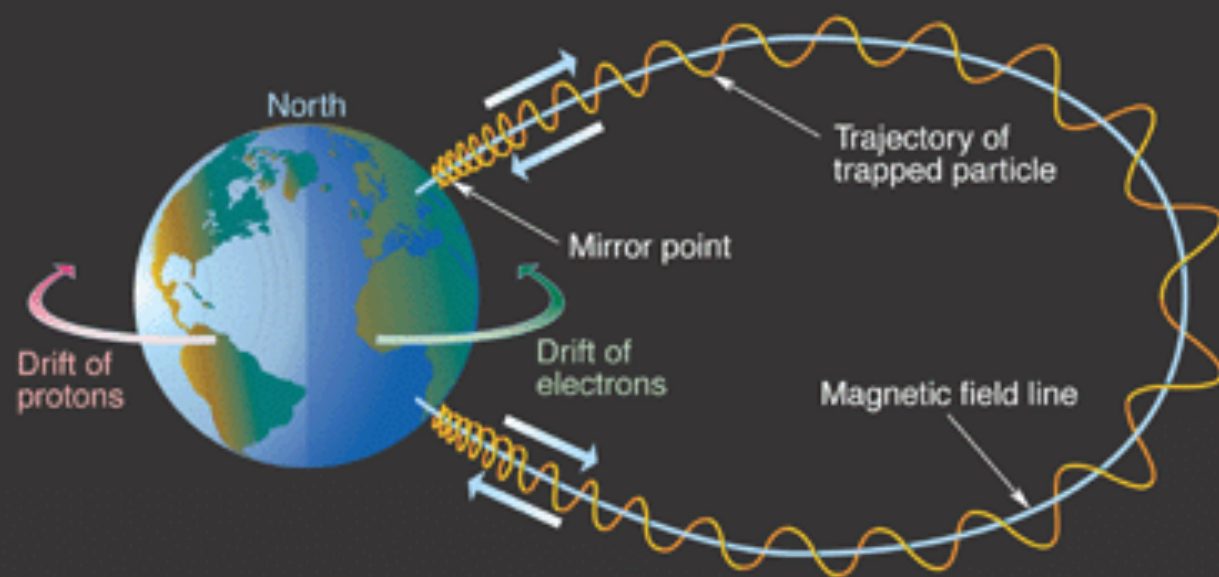
Solar modulation



Earth magnetosphere



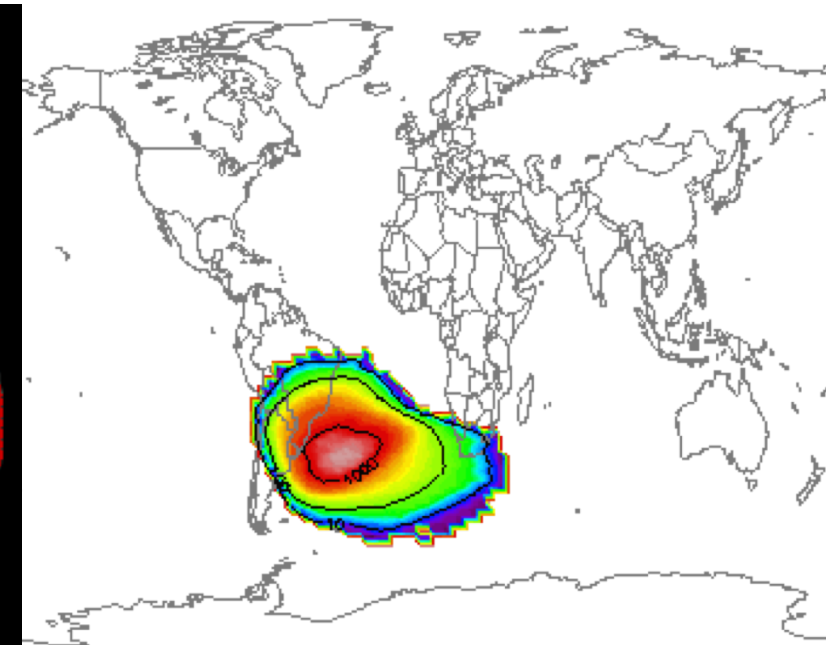
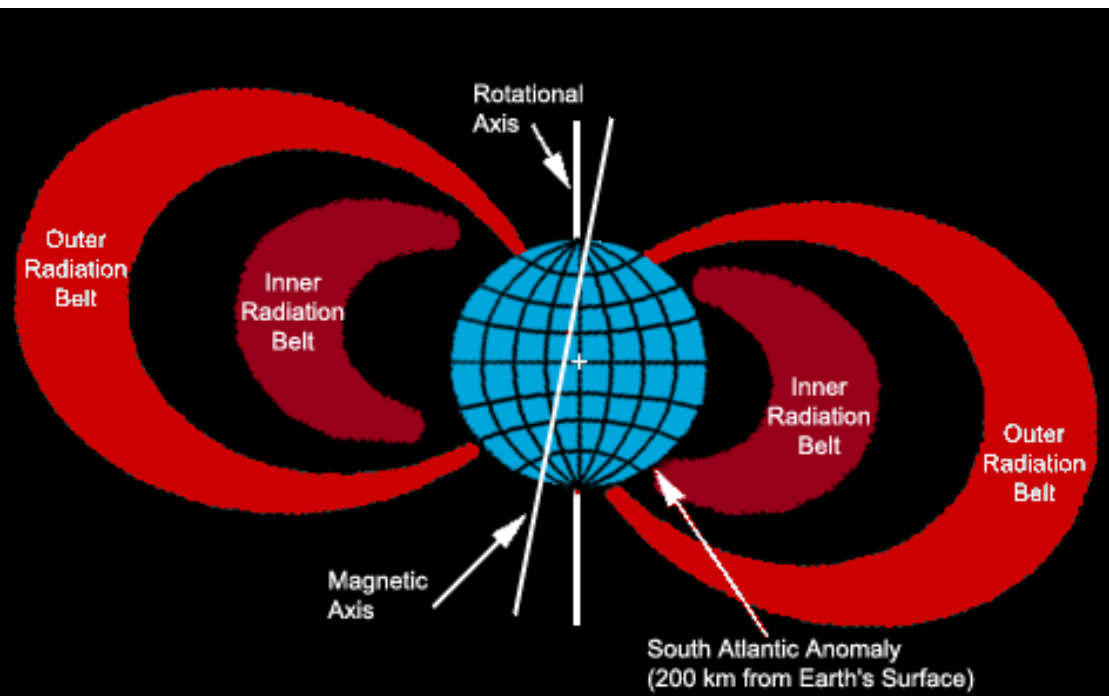
Earth magnetosphere



Charged particles (if not too energetic) are trapped in the **Radiation Belts**

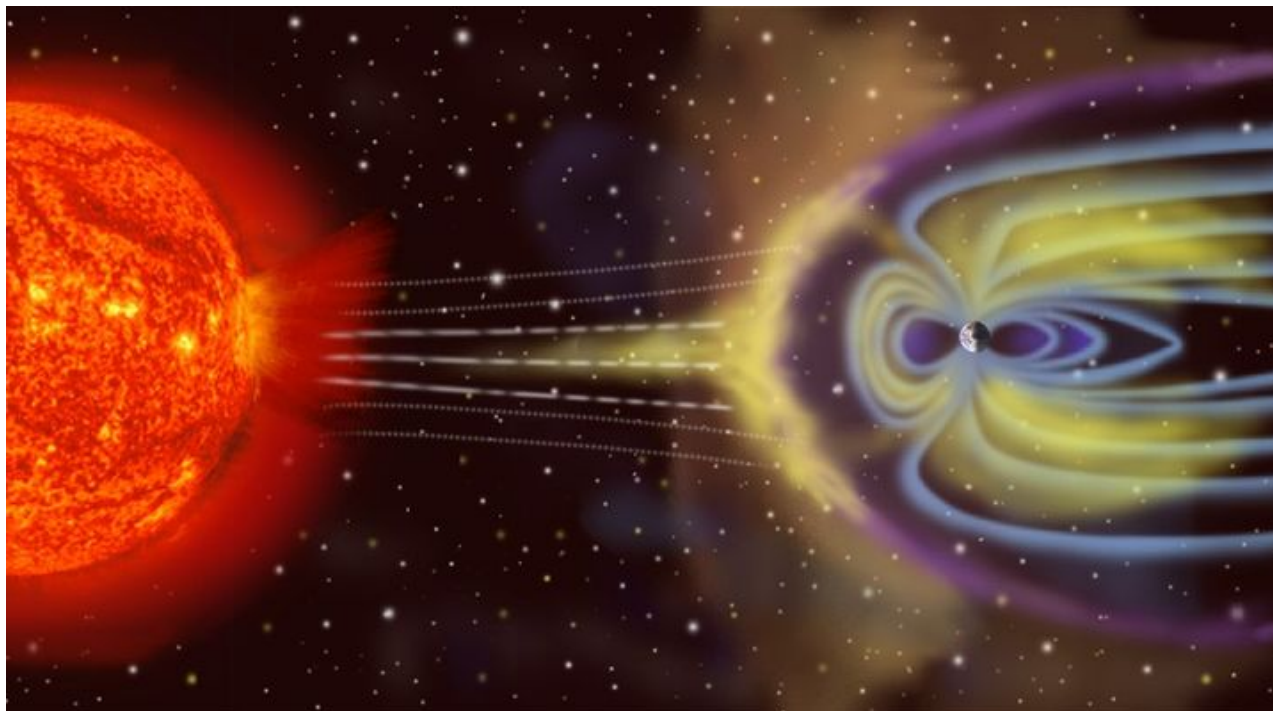
Radiation belts and satellite orbits

The **Earth magnetic field** protects many **satellites** and the International Space Station from (relatively low energy) charged particles, since they are in a **Low Earth Orbit (LEO)** (400-600 km height; ~90 minutes period), below the **Radiation Belts**



Space environment above the belts

Satellites in **High Earth Orbit (HEO)** and interplanetary probes are exposed to a much **higher dose** and **variable flux** of charged particles: higher instrumental and electronic **background**, degradation of electronics, solar panels and scientific instruments, higher probability of electronic failures or glitches



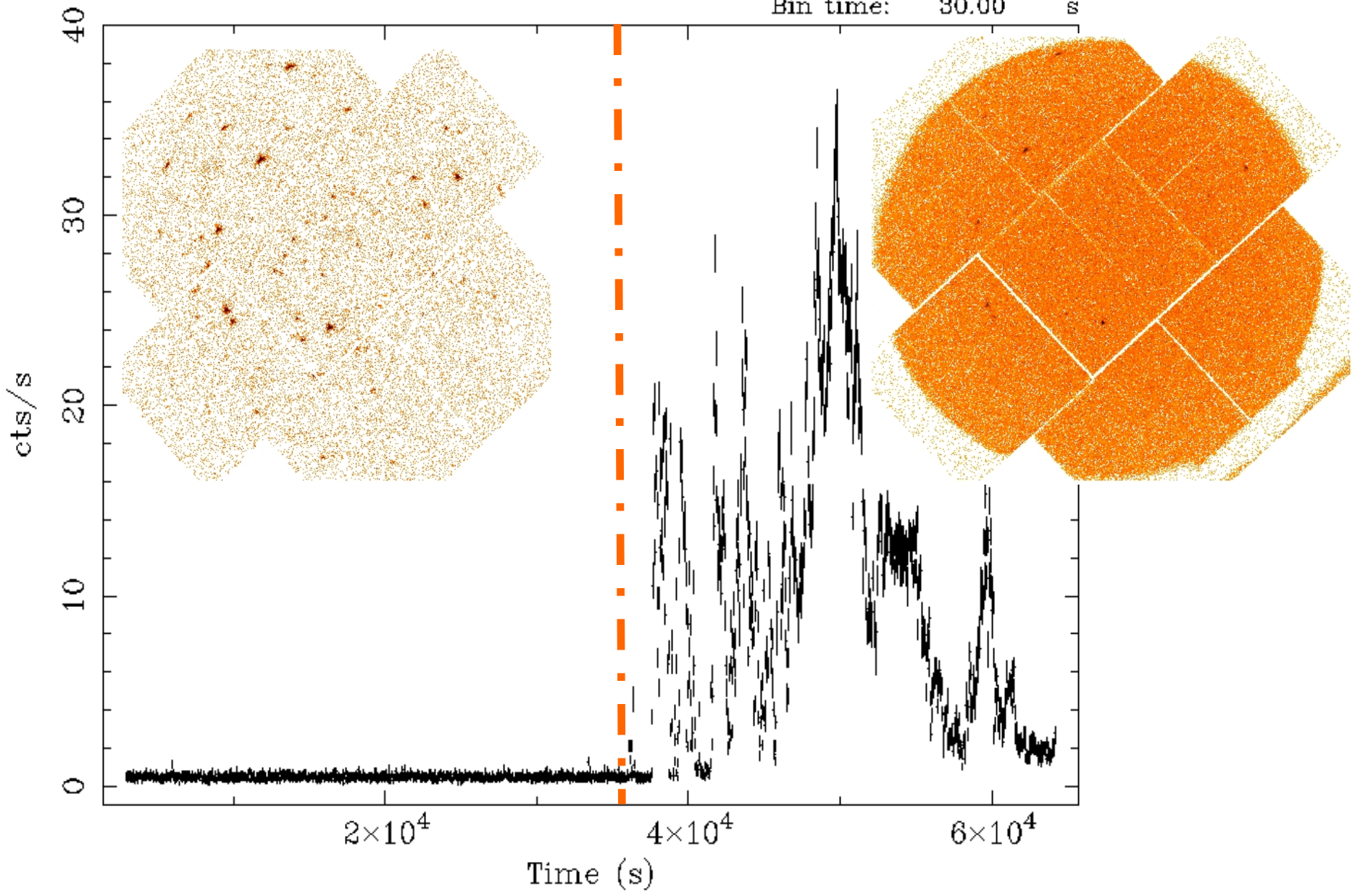
Sensitivity

The **sensitivity** of an astronomical instrument is its ability to detect **faint objects** (in sufficiently long observations).

An instrument with a large effective area is not necessarily more sensitive, because the instrumental **background** must also be considered. *For example*, good **spatial resolution** makes an instrument more sensitive (for point-like sources).

Lockman Hole (MOS2; 0.5–10 keV)

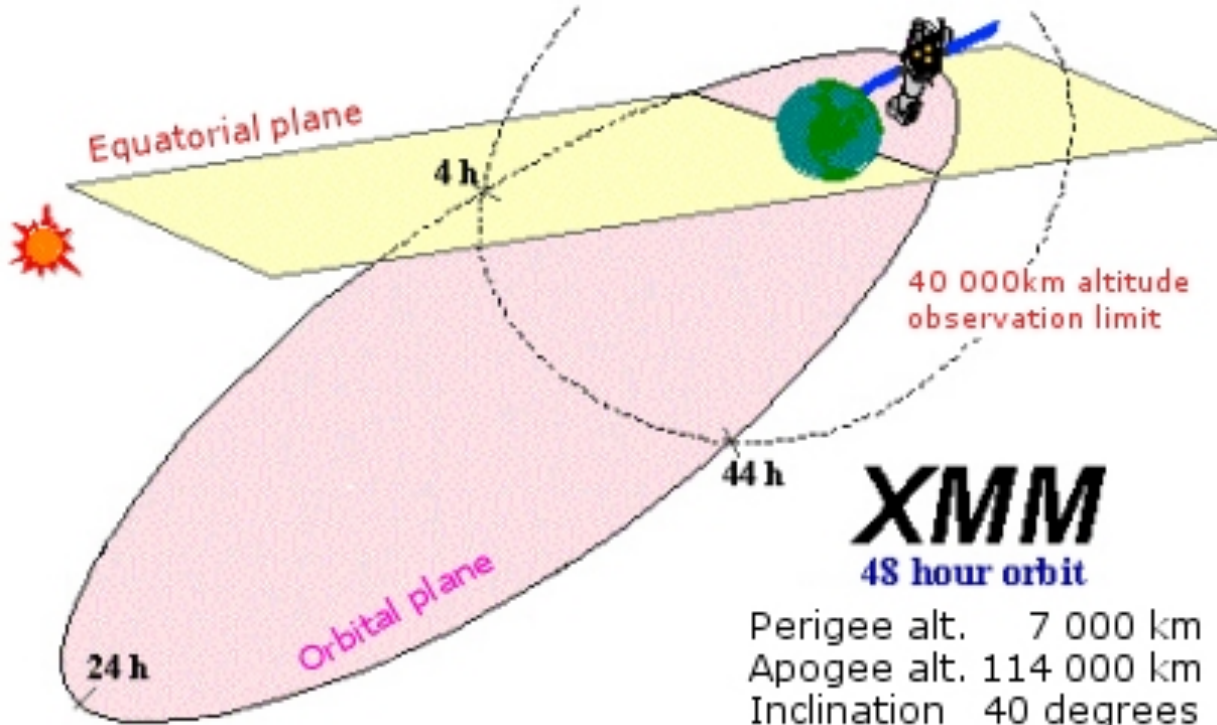
Bin time: 30.00 s



Start Time 2000-04-26T03:48:58

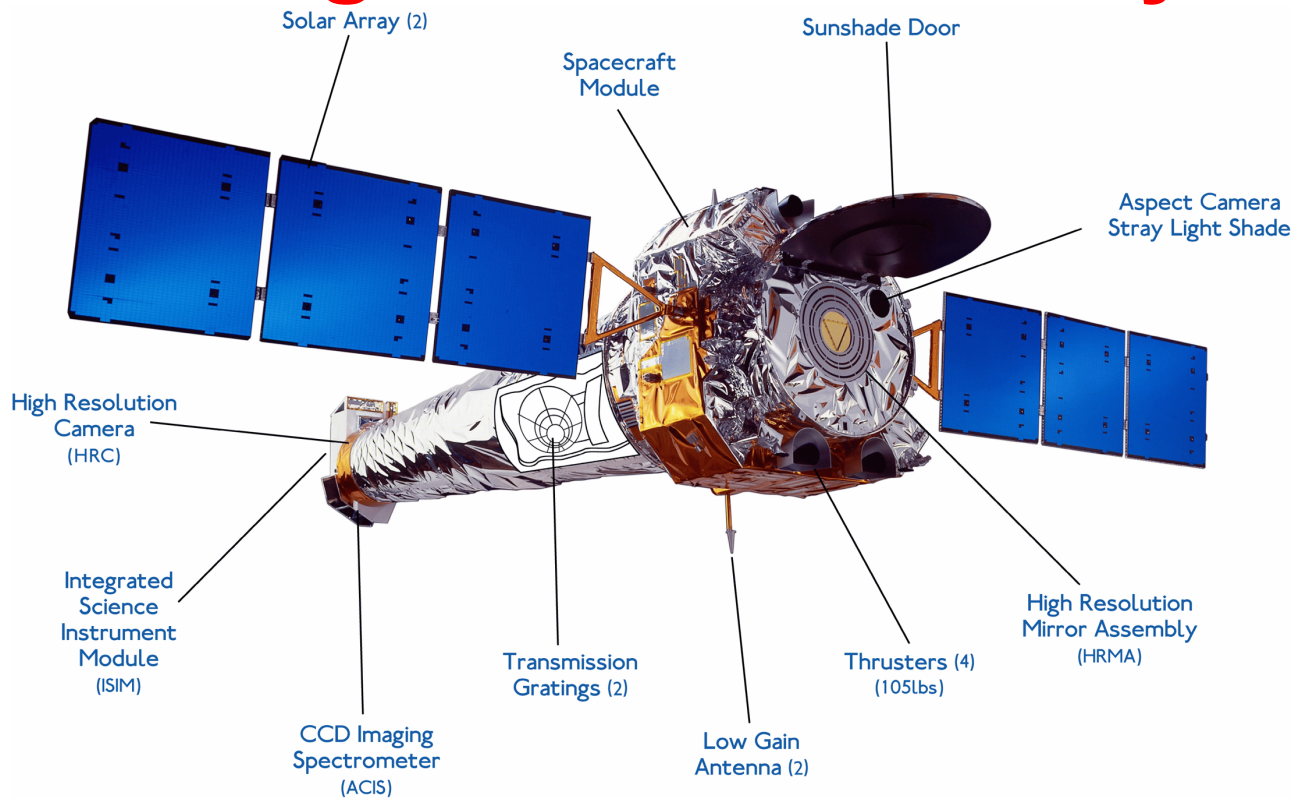
Stop Time 2000-04-26T20:49:58

XMM-Newton orbit (HEO)



- Particle flares in *XMM-Newton* reduce usable **observing time** (or data quality)
- All X-ray telescopes in **LEO** are not affected by particle background flares because they are **screened by radiation belts** ⇒ **charged particles**

Chandra: high resolution X-ray images



Launched by NASA a few months before *XMM-Newton*, ***Chandra*** is also in HEO orbit:

- Particle **background flares**
- ACIS-I **CCDs damaged** by high dose received during first passages through radiation belts

Previous ESA X-ray mission, **EXOSAT** (1983-1986),
was in **HEO** and had an instrument with **X-ray mirrors**

Serendipitous *EXOSAT* sources in the region of the Coma cluster: Active Galactic Nuclei with steep X-ray spectra

G. Branduardi-Raymont and K. O. Mason *Mullard Space*

*Science Laboratory, University College London, Holmbury St Mary, Dorking, Surrey RH5
6NT*

P. G. Murdin *Royal Greenwich Observatory, Herstmonceux Castle, Hailsham, East
Sussex BN27 1RP*

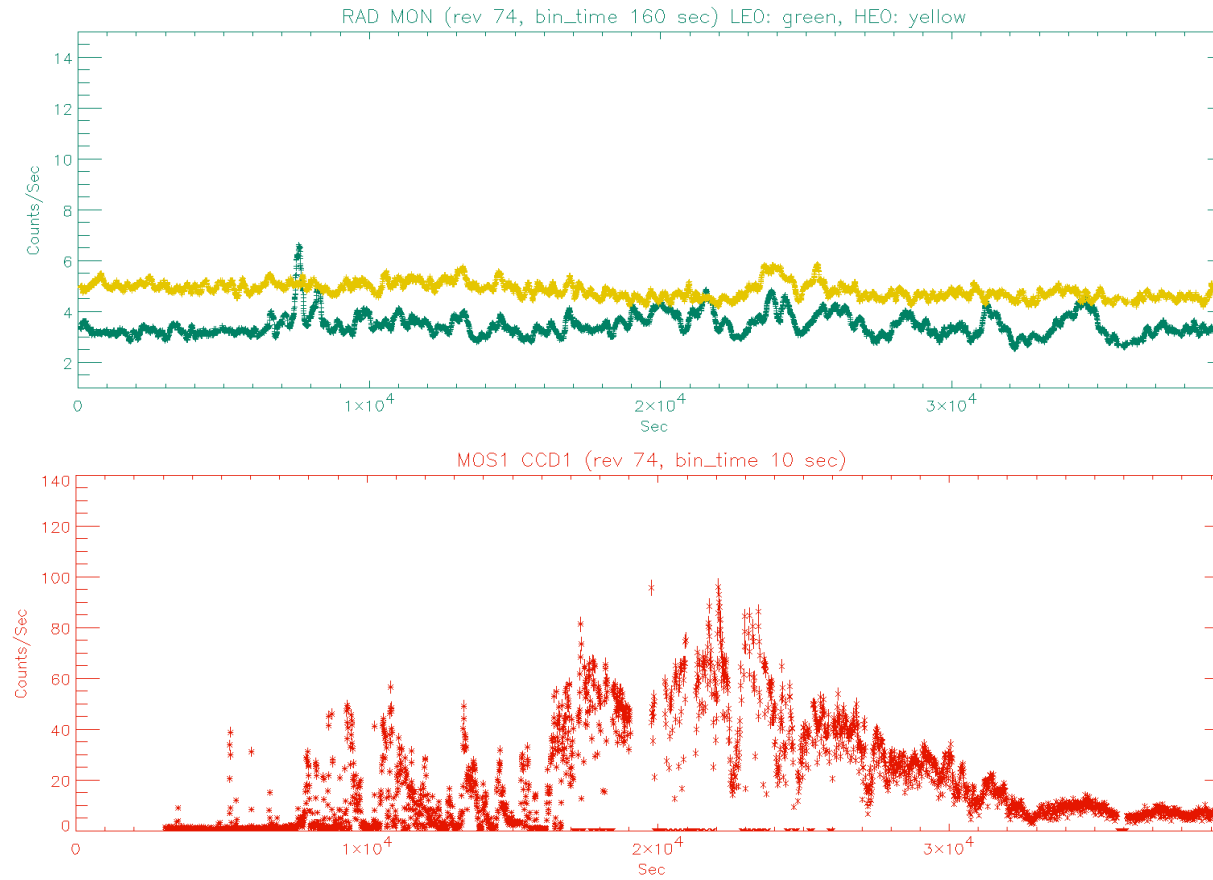
C. Martin *Instituto de Astrofisica de Canarias, La Laguna, Spain*

Accepted 1985 June 17. Received 1985 June 14; in original form 1985 May 16

large part of it is contaminated by an abnormally high level of particle background (usually this is a consequence of enhanced solar activity) and has not been used in the analysis reported here; its inclusion does not modify the results, but only increases the noise level of the image data.

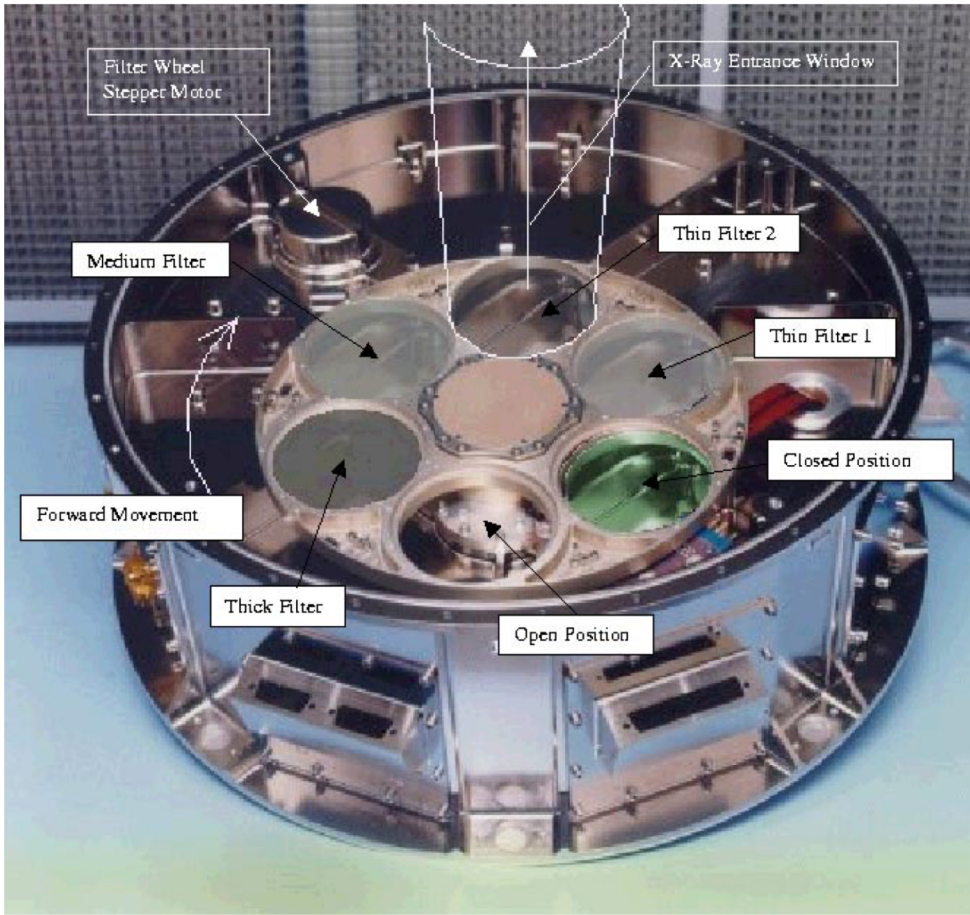
⇒ background particles are **focussed by the mirrors**

Which particles cause the flares?

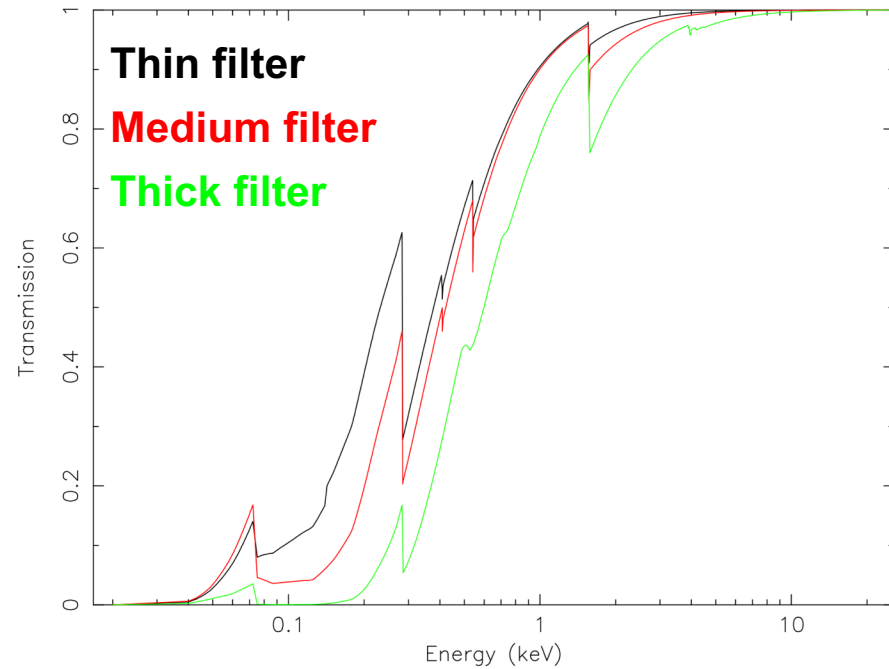


XMM-Newton background flares have **no correlation** with flux in its **Radiation Monitor** (8-40 MeV protons)

XMM/EPIC filters

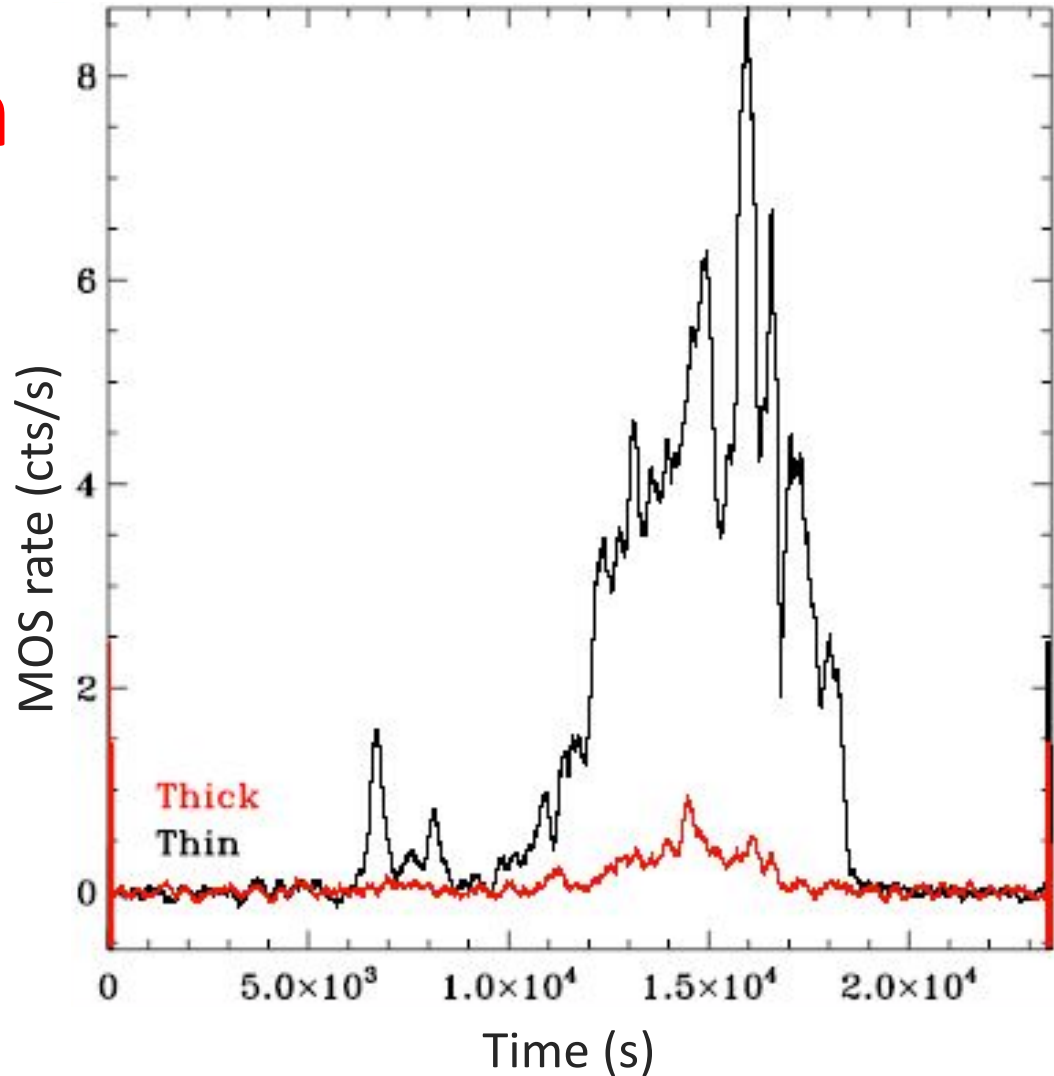


X-ray **CCDs** are sensitive to **optical/UV** light reflected by **X-ray mirrors** \Rightarrow Optical blocking **filters**

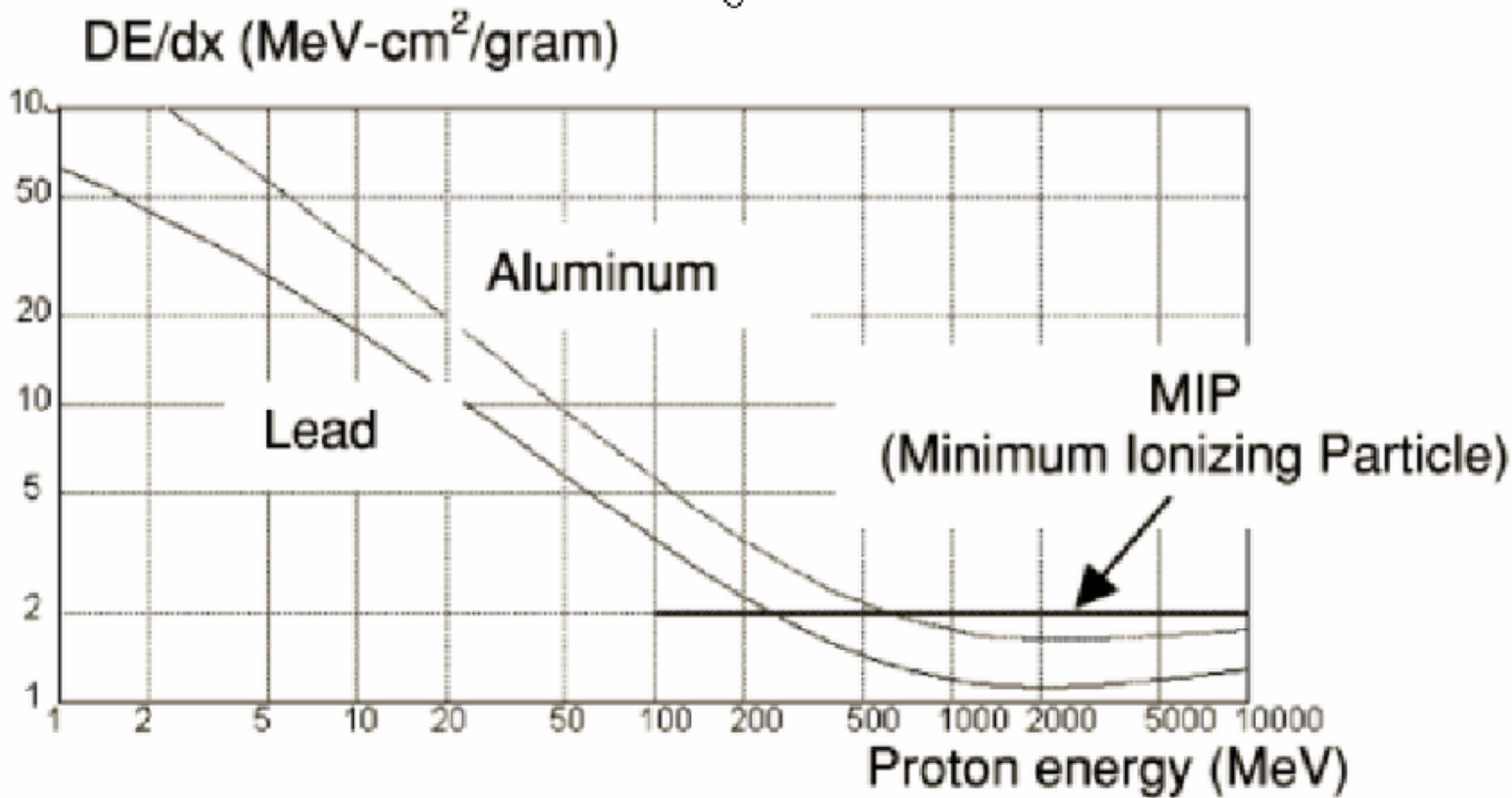


Effect of filters on particle flares

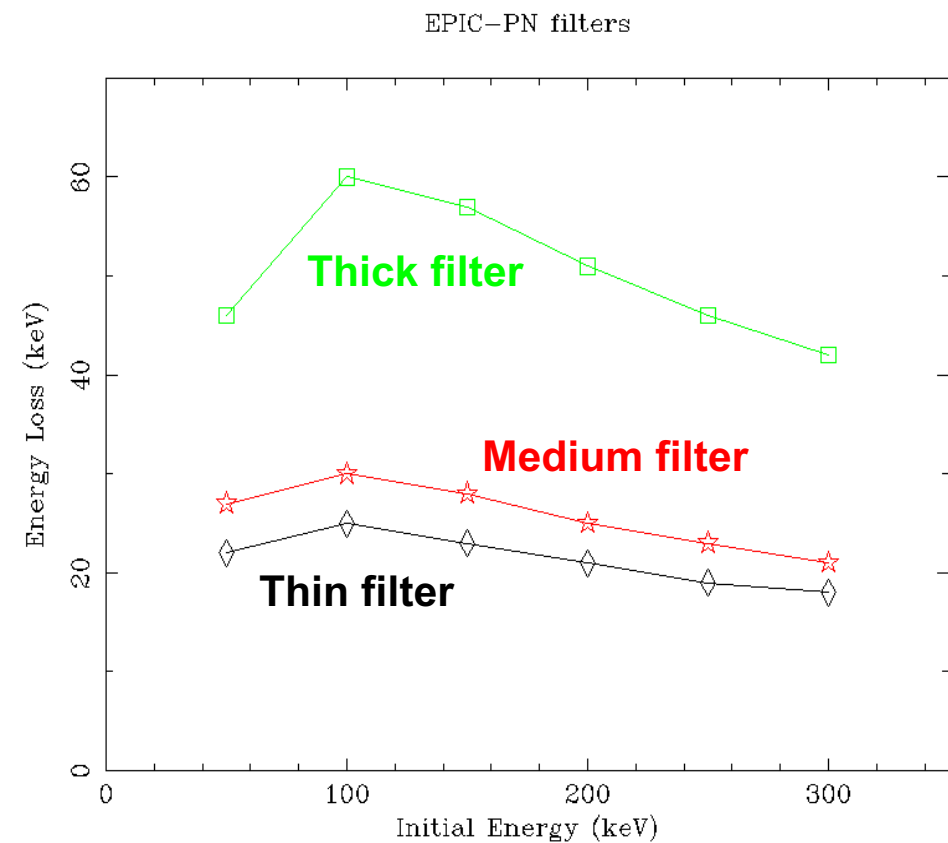
MOS1/MOS2 cameras simultaneously observing the same flaring episode with **different filters** detect substantially **different count rates**



Proton energy loss



Proton energy loss in EPIC filters

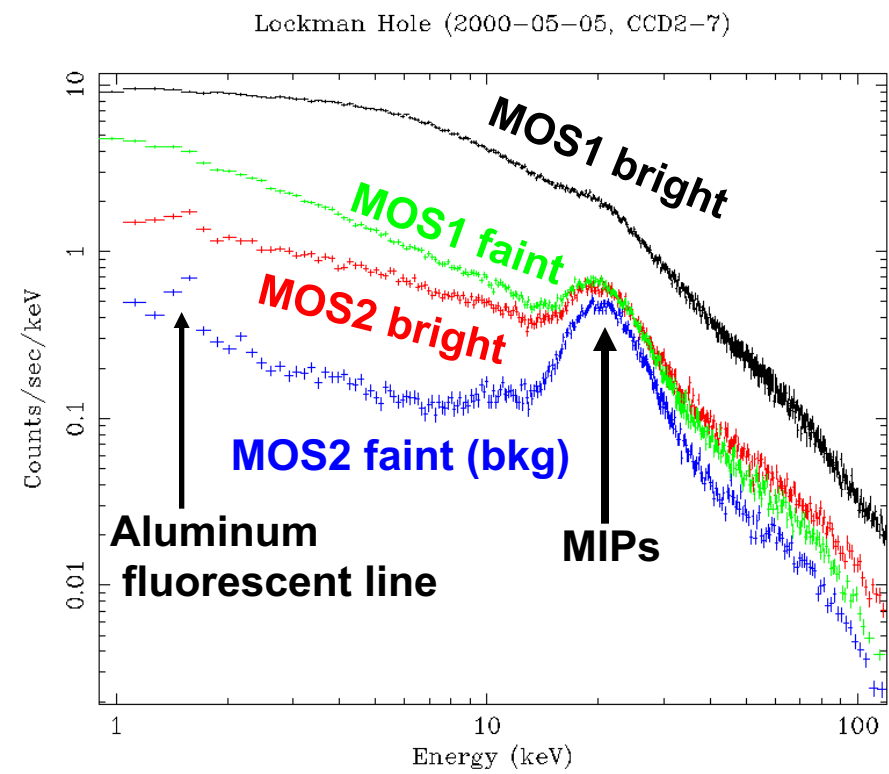
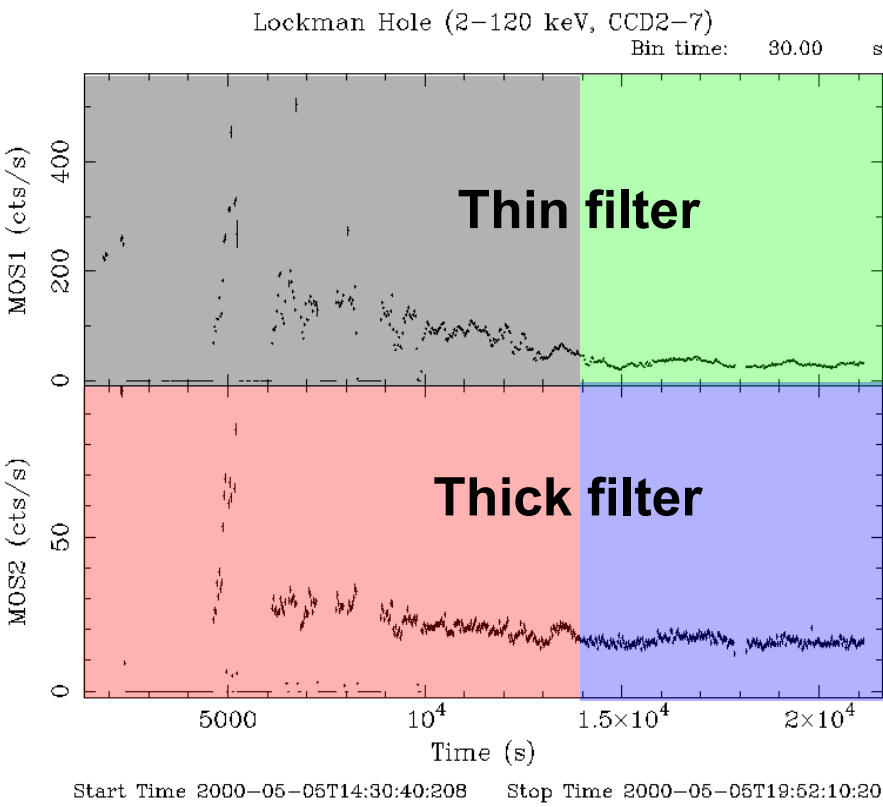


- Due to **energy loss**, protons above threshold become detectable
- **Filters** stop low energy protons
- **Thick filter** stops protons up to higher energies

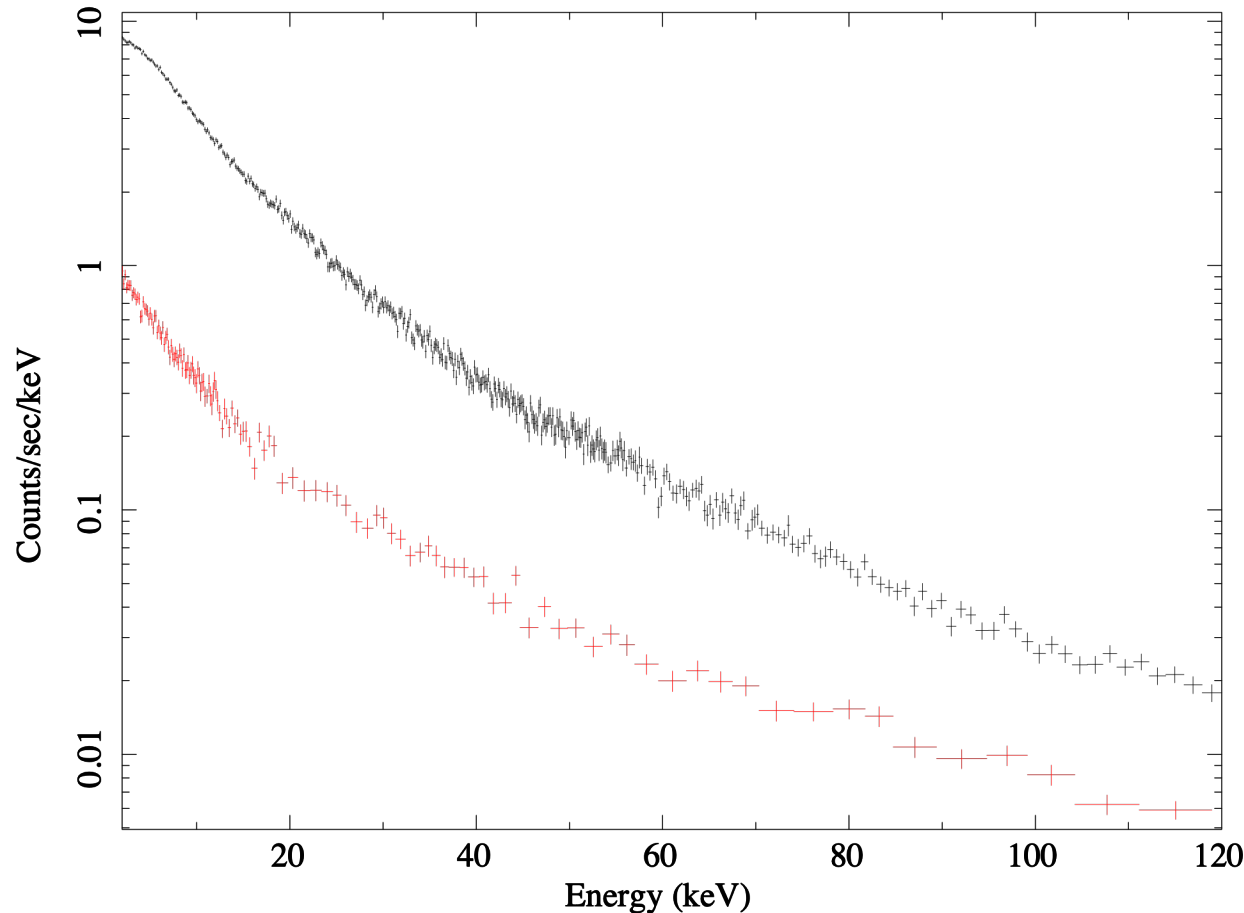
Proton spectrum is soft ⇒ reduced background

MOS with thin/thick filter

- MOS in low gain mode (0.2-12 keV \rightarrow 2-120 keV)
- Background from faint time period



Spectra with Thin and Thick filter

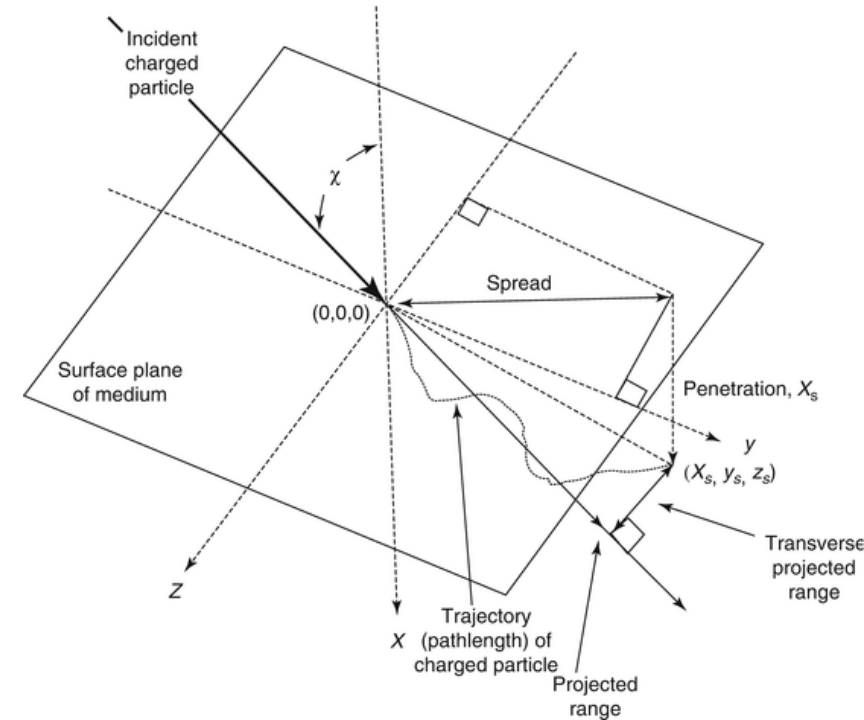
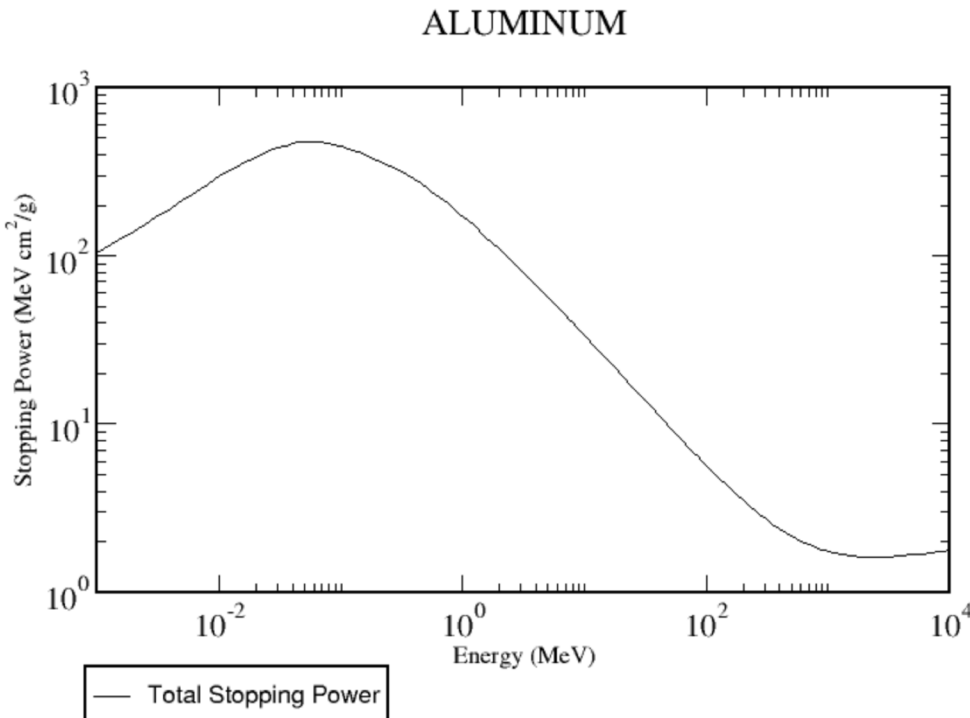


$\Delta E \approx 40 \text{ keV}$ (for $E > 20 \text{ keV}$)

Proton energy loss in filters

- MOS **thin** filter: 0.16 μm polyimide + 0.04 μm Al
- MOS **thick** filter: 0.33 μm polypropylene + 0.11 μm Al + 0.045 μm tin
- **Proton** energy loss from *NIST Standard Reference Database 124 (considering also Detour Factor)*

<https://physics.nist.gov/PhysRefData/Star/Text/PSTAR.html>



Proton energy loss in filters

- MOS **thin** filter: 0.16 μm polyimide + 0.04 μm Al
- MOS **thick** filter: 0.33 μm polypropylene + 0.11 μm Al + 0.045 μm tin
- **Proton** energy loss from *NIST Standard Reference Database 124 (considering also Detour Factor)*

<https://physics.nist.gov/PhysRefData/Star/Text/PSTAR.html>

(required) Kinetic Energy (MeV)	Stopping Power (MeV cm^2/g)			Range		
	Electronic	Nuclear	Total	CSDA (g/cm^2)	Projected (g/cm^2)	Detour Factor Projected / CSDA
1.000E-03	9.238E+01	1.197E+01	1.043E+02	1.471E-05	3.758E-06	0.2555
1.500E-03	1.131E+02	1.072E+01	1.239E+02	1.906E-05	5.590E-06	0.2933
2.000E-03	1.306E+02	9.749E+00	1.404E+02	2.285E-05	7.413E-06	0.3245
2.500E-03	1.461E+02	8.967E+00	1.550E+02	2.623E-05	9.205E-06	0.3509
3.000E-03	1.600E+02	8.324E+00	1.683E+02	2.933E-05	1.096E-05	0.3738
4.000E-03	1.848E+02	7.322E+00	1.921E+02	3.487E-05	1.438E-05	0.4122
5.000E-03	2.066E+02	6.571E+00	2.131E+02	3.981E-05	1.765E-05	0.4434
6.000E-03	2.263E+02	5.982E+00	2.323E+02	4.430E-05	2.080E-05	0.4696
7.000E-03	2.444E+02	5.505E+00	2.499E+02	4.845E-05	2.384E-05	0.4921
8.000E-03	2.613E+02	5.110E+00	2.664E+02	5.232E-05	2.677E-05	0.5117
9.000E-03	2.771E+02	4.775E+00	2.819E+02	5.597E-05	2.961E-05	0.5291
1.000E-02	2.921E+02	4.488E+00	2.966E+02	5.943E-05	3.236E-05	0.5445
1.250E-02	3.206E+02	3.917E+00	3.245E+02	6.746E-05	3.895E-05	0.5773
1.500E-02	3.448E+02	3.491E+00	3.483E+02	7.489E-05	4.523E-05	0.6040
1.750E-02	3.657E+02	3.157E+00	3.689E+02	8.186E-05	5.127E-05	0.6263
2.000E-02	3.838E+02	2.889E+00	3.867E+02	8.848E-05	5.711E-05	0.6454
2.250E-02	3.996E+02	2.667E+00	4.022E+02	9.481E-05	6.277E-05	0.6620
2.500E-02	4.132E+02	2.480E+00	4.157E+02	1.009E-04	6.829E-05	0.6767

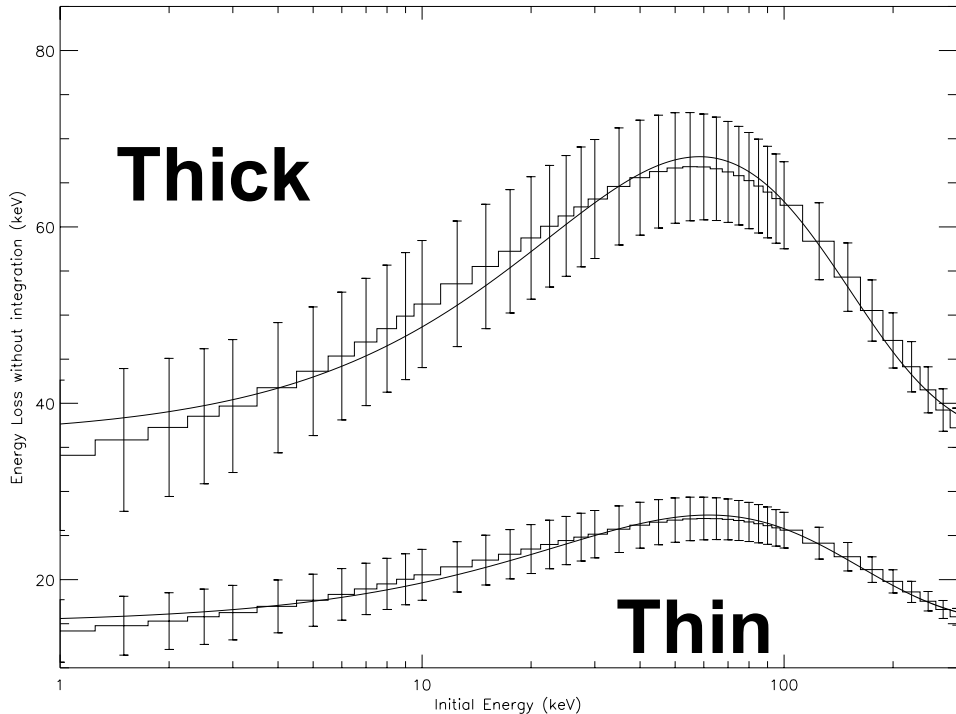
Continuous
Slowing Down
Approximation
range ($d \cdot \rho$)

ΔE
 $\Delta d \cdot \rho$

Proton energy loss in filters

- Constructing the **energy loss for each filter** as if protons keep the same energy across the filter (only valid for small energy losses, i.e., **short tracks**)
- Empirical **model** of energy loss for each filter using:

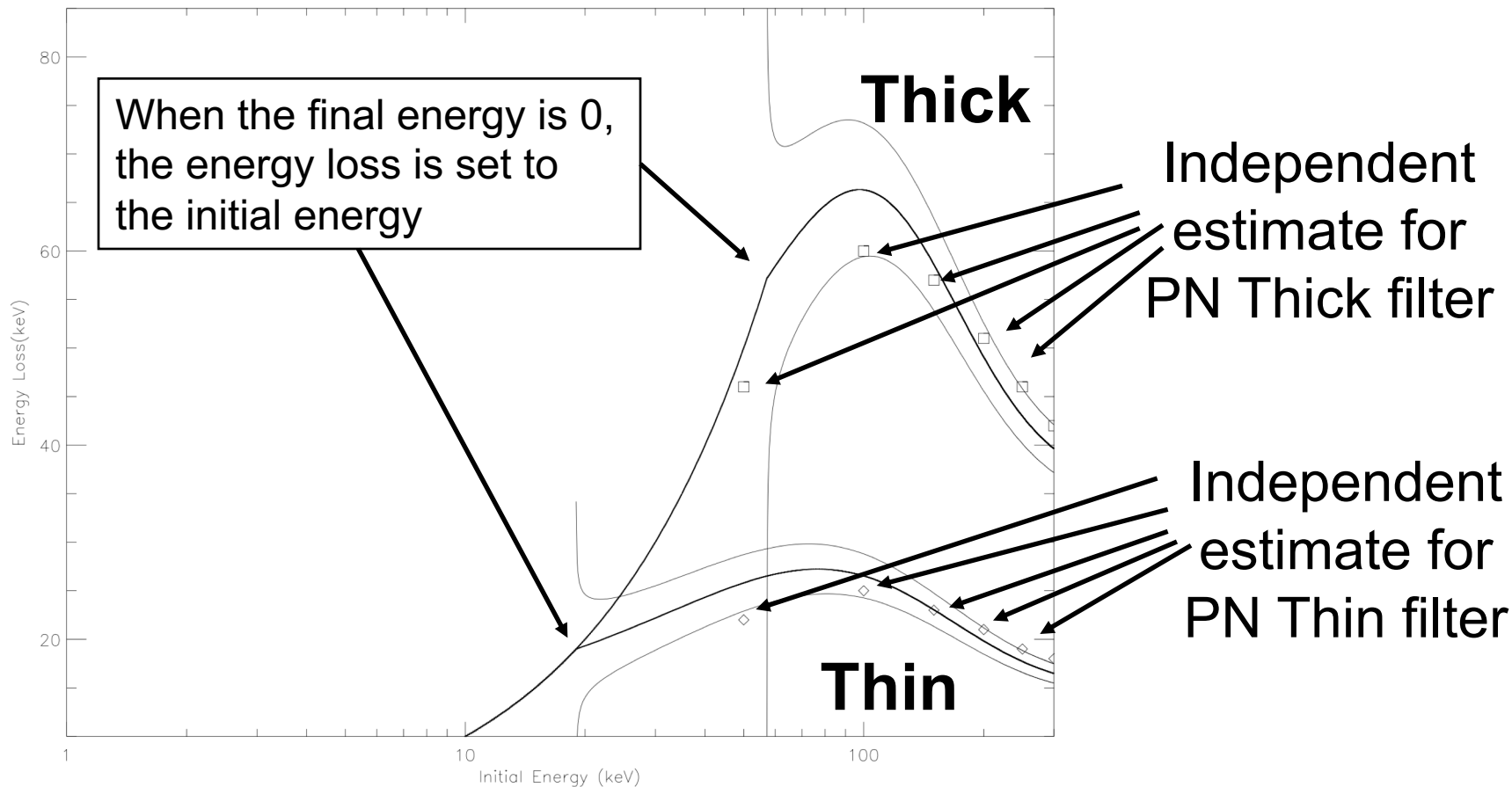
$$dE(E) = \Delta E + c \cdot E \cdot \exp(-E/E_f)$$



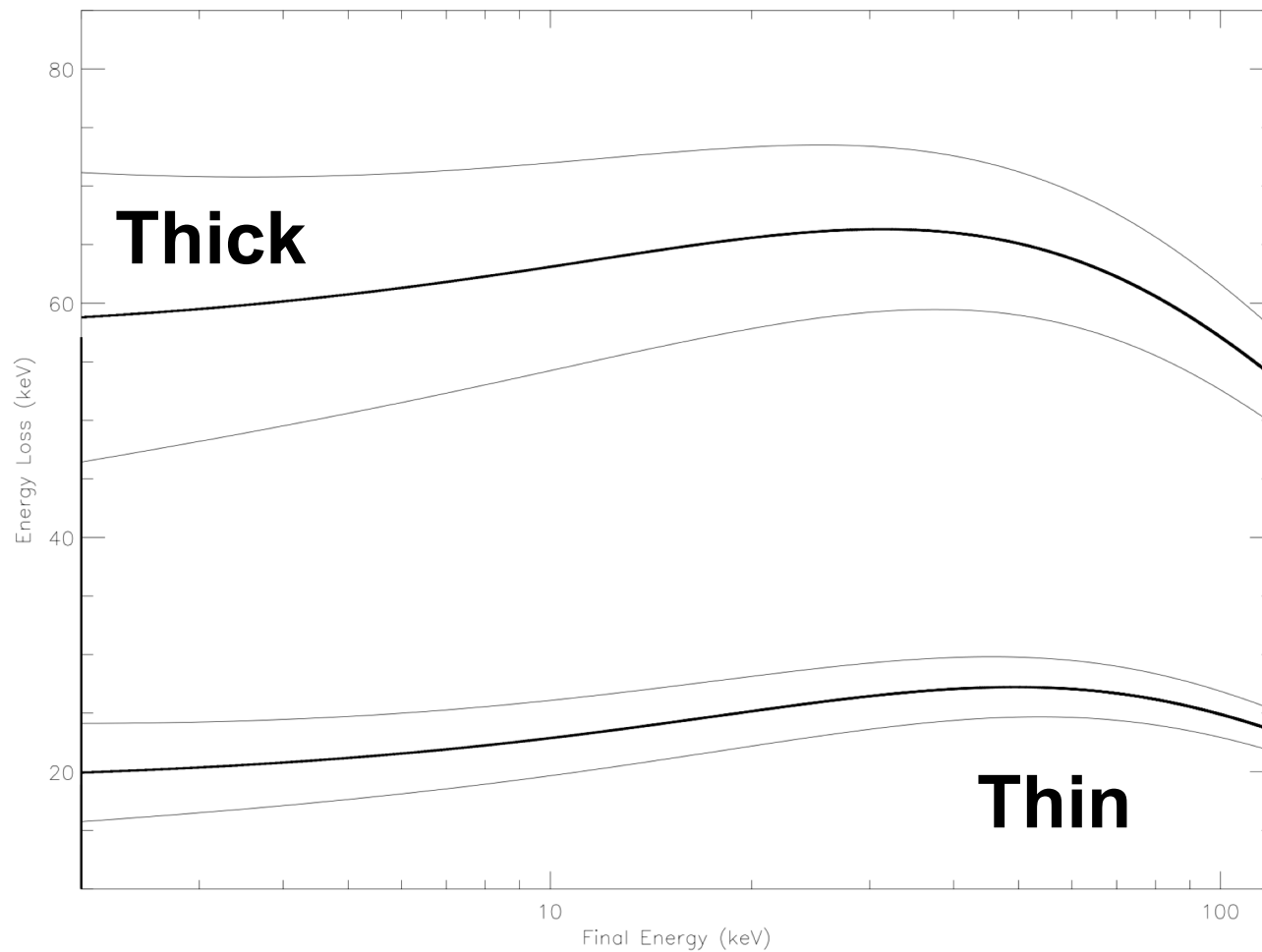
$\Delta E_{\text{thin}} = 15 \pm 2 \text{ keV}$,
 $C_{\text{thin}} = 0.5 \pm 0.1$,
 $E_{f,\text{thin}} = 62 \pm 12 \text{ keV}$,
 $\Delta E_{\text{thick}} = 36 \pm 5 \text{ keV}$,
 $C_{\text{thick}} = 1.5 \pm 0.4$,
 $E_{f,\text{thick}} = 58 \pm 11 \text{ keV}$,

Proton energy loss in filters

- We divide the filter thickness into **1000 bins**, where the **energy loss is constant** between the initial and final energy and we **integrate** the energy loss



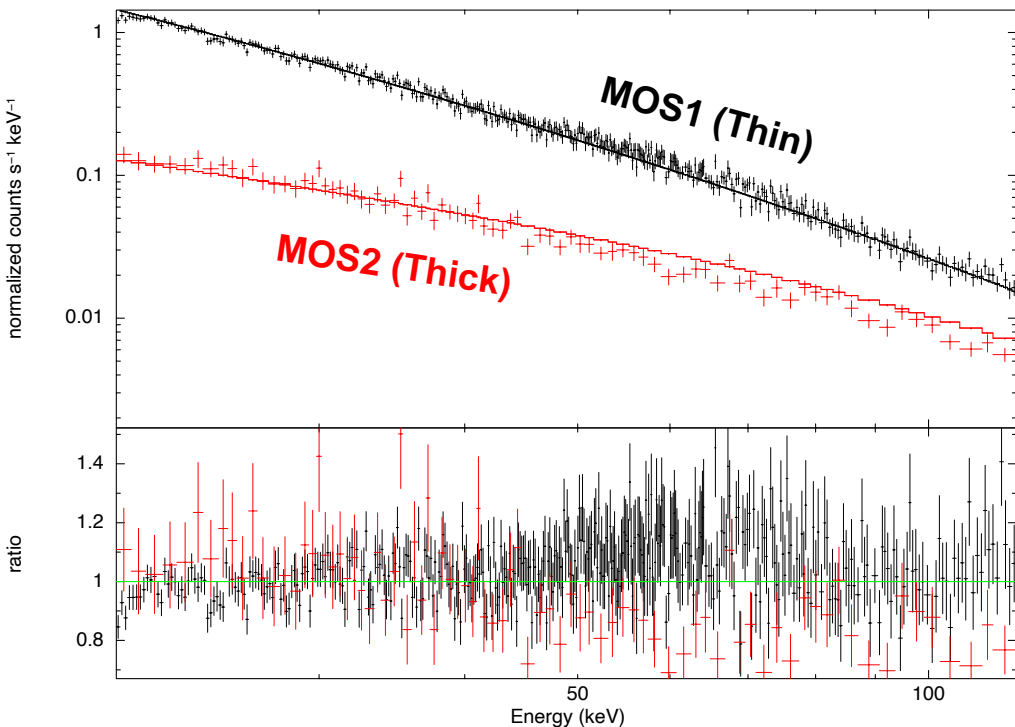
Proton energy loss in filters



The energy loss **only slightly depend on energy**
if the final energy is in the 2-120 keV range

MOS spectra: simultaneous fit

- Background subtracted spectra with diagonal response matrix
- Restricted to 20-120 keV band



Model:

$$F(E) = k \cdot (E + \Delta E)^{-\alpha}$$

$$\begin{aligned}\alpha &= 3.9 \pm 0.1, \\ \Delta E_{\text{thin}} &= 25.5 \pm 2 \text{ keV}, \\ \Delta E_{\text{thick}} &= 65.5 \pm 2 \text{ keV}, \\ \chi^2_{\text{red}} &= 1.11 / 612 \text{ d.o.f.}\end{aligned}$$

Proton energy loss in filters

